COMPDYN 2021
8th ECCOMAS Thematic Conference on
Computational Methods in Structural Dynamics and Earthquake Engineering
M. Papadrakakis, M. Fragiadakis (eds.)
Streamed from Athens, Greece, 27–30 June 2021

# A NUMERICAL STUDY ON A TIMBER-BASED SEISMIC RETROFIT INTERVENTION FOR MASONRY INFILLED CONCRETE FRAMES

**F. Smiroldo**[1], **D. Viel**[2], **I. Giongo**[1], **and M. Piazza**[1]

[1] University of Trento
Via Mesiano 38123, Trento (Italy)
{francesco.smiroldo, ivan.giongo, maurizio.piazza}@unitn.it

[2] University of Trento
Via Mesiano 38123, Trento (Italy)
davide.viel@alumni.unitn.it

## Abstract

*The paper focuses on a retrofit strategy applicable to existing reinforced concrete (RC) frame structures to reduce their seismic vulnerability. The intervention strategy, for the sake of brevity named RC-TP (Reinforced Concrete-Timber Panels), consists in the removal of the existing masonry infills and in their replacements with Cross Laminated Timber (CLT) panels fixed to the concrete elements by means of a timber subframe and a dissipative connection comprised of metal dowel-type fasteners. The analyses were performed via finite element modelling by adopting numerical strategies with different levels of refinement. In particular, refined 3-dimensional models (created using the software Abaqus) and simpler 2-dimensional models (created using the software SAP2000) were used. At first, the refined modelling approach was validated on experimental evidence on timber and concrete connectors available from the literature. Then, such 3-dimensional models were used to investigate the connection system of the proposed retrofit strategy paying particular attention to possible out-of-plane effects that cannot be directly observed with 2-dimensional models. The obtained results were used to calibrate the 2-dimensional models so that these "secondary" effects could be accounted for even in the simplified modelling. Subsequently, both modelling approaches were used to analyse an isolated one-storey one-bay frame via nonlinear static analyses that addressed the a) bare, b) original masonry infilled, and c) retrofitted configurations. The two alternative numerical strategies showed consistent results, both suggesting that the proposed intervention can significantly improve the seismic behaviour of existing RC frames.*

**Keywords:** Structural rehabilitation; Seismic engineering; Concrete structures; Timber panels; Finite-element modelling; Nonlinear analyses.

# 1 INTRODUCTION

Reinforced concrete (RC) buildings represent a large percentage of the built heritage stock of many countries. Over the last decade, numerous studies have shown that, even in the case of minor earthquakes, past construction practices often led to vulnerabilities that resulted in extensive damage and collapse of the RC structure or portions of it [1], [2]. Examples of such vulnerabilities are the collapse of the masonry infills, the brittle shear failure of the RC elements or the activation of soft-storey mechanisms. Most of these buildings, indeed, were designed using codes that when they did not neglect the seismic action, accounted for it only partially. In addition, the presence of masonry infills was often disregarded in the modelling phase although nowadays it is well-known that their presence has a strong influence on the seismic behaviour of the structure [3], [4].

As a consequence, the interest of the scientific community towards such issues has grown over the years, with new solutions to improve the seismic behaviour of RC structures being proposed more and more frequently. Among these, the solutions that see the use of timber elements are gaining attention (e.g., [5]-[8]). In this regard, a retrofit intervention presented by Smiroldo et al. [9], [10] is being developed at the University of Trento (Italy). Such intervention strategy aims at mitigating the seismic vulnerability of existing RC structures without modifying the original structural system. The intervention, named RC-TP (Reinforced Concrete-Timber Panels), consists in the removal of the existing masonry infills and in their replacement with Cross Laminated Timber (CLT) structural panels connected to the existing RC frame so as to redistribute the stresses due to the seismic action in order to avoid the development of brittle collapses and to favour the development of ductile mechanisms.

In this paper, the RC-TP retrofit strategy was studied via finite element modelling by adopting numerical strategies with two different levels of refinement: a 3-dimensional (3D), refined modelling approach was developed by using the finite element software Abaqus [11], while a 2-dimensional (2D), simpler approach was developed using the software SAP2000 [12]. In the first phase, the refined approach was calibrated on experimental evidence from the literature [13]-[15] concerning concrete and timber-to-timber connections. Then, the 3D approach was used to reproduce the connection details implemented in the proposed intervention. Starting from the outcomes of the refined 3D models and focusing on the observed out-of-plane secondary effects that could have not been explicitly reproduced by 2-dimensional models, the 2D approach was tweaked to take implicitly into account such effects. Subsequently, the analyses were extended to more complex models of multiple-fastener connections and then to complete one-storey, one-bay RC frames retrofitted with the RC-TP intervention. The frame was analysed also considering the “bare frame” and “original masonry-infilled” configurations. Both in the refined and in the simplified approach, the masonry infills were simulated with modelling strategies adapted from the literature [16]-[18].

In all the configurations analysed, the alternative modelling approaches led to consistent results and confirmed the ability of the proposed intervention system to enhance the seismic behaviour of existing RC frames.

## 2 PRE-INTERVENTION RC FRAME

The intervention system presented in this paper is designed to be applied to existing structures. Consequently, the geometry, the detailing and the material properties of the case-study RC frame and masonry infill were selected so as to reflect the typical characteristics of buildings belonging to the existing stock. Table 1 reports the mechanical properties assumed for concrete (frame elements), steel (rebars and confinement reinforcement) and masonry (infills) in the numerical models.

| **Concrete** | | **Steel** | | **Masonry** | | |
|---|---|---|---|---|---|---|
| $f_c$ [MPa] | $E_c$ [MPa] | $f_y$ [MPa] | $E_s$ [MPa] | $f_m$ [MPa] | $f_{v,0}$ [MPa] | $E_m$ [MPa] |
| 16,73 | 25673 | 440 | 210000 | 6,00 | 0,25 | 3000 |

Table 1: Mechanical properties of existing materials

Table 2 reports the geometrical and load characteristics of the RC frame used in the numerical analyses, where *n* is the number of longitudinal rebars, *Φ* is the diameter of rebars in millimetres and @ is the stirrup spacing in millimetres.

| **Pre-intervention characteristics** | | **Value** |
|---|---|---|
| Concrete frame | Length *l* [mm] | 5000 |
| | Height *h* [mm] | 3000 |
| | Column section (base × height) [mm] | 300 × 300 |
| | Beam section (base × height) [mm] | 300 × 500 |
| Reinforcements | Column longitudinal rebars | *n*3+3 *Φ*16 |
| | Column confinement reinforcement (2-legged stirrups) | *Φ*6 @150 |
| | Beam longitudinal rebars at ends (top – bottom side) | 6 *Φ*14 – 4 *Φ*14 |
| | Beam longitudinal rebars at mid-span (top – bottom side) | 2 *Φ*14 – 4 *Φ*14 |
| | Beam confinement reinforcement (2-legged stirrups) | *Φ*6 @200 |
| Masonry infill | Thickness [mm] | 200 |
| Loads | Vertical distributed (upper beam) [kN/m] | 10 |
| | Vertical concentrated (each column) [kN] | 100 |

Table 2: Geometrical and load pre-intervention characteristics

## 3 INTERVENTION SYSTEM

Because the proposed intervention strategy has been fully illustrated in [9] and [10], in the present paper, only a brief description is reported. Starting from the masonry-infilled original configuration (Figure 1a), the first step is the removal of the masonry infill (Figure 1b).

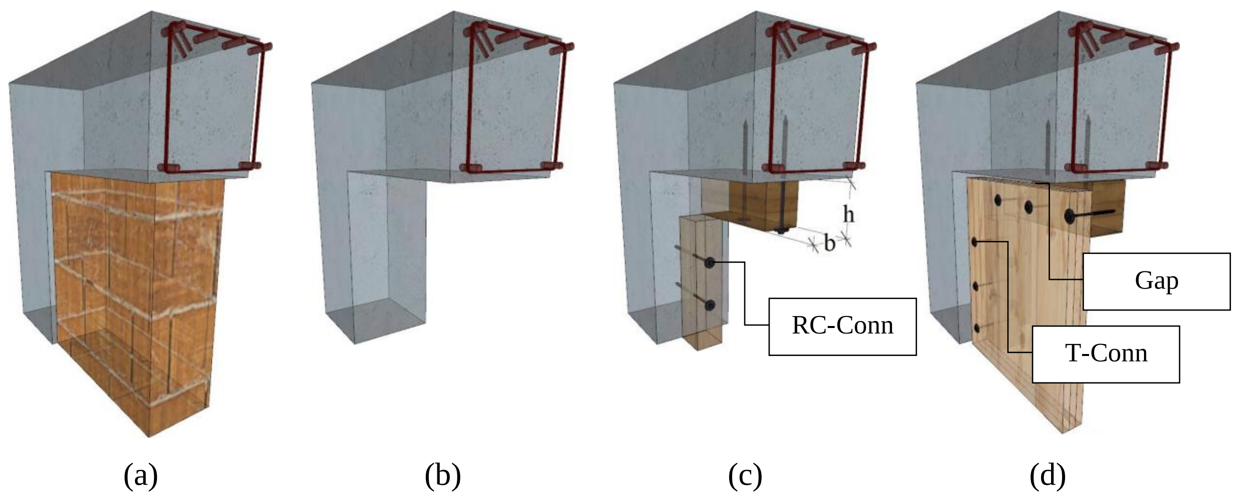


Figure 1: Intervention procedure

Subsequently, a timber subframe is connected to the RC elements through metal screw fasteners (Figure 1c). This connection is reported in Figure 2 and is named "RC-Conn" for the sake of brevity. It comprises partially-threaded concrete screws (named RC-F), inserted with washers (RC-W). The fasteners are regularly spaced at 15 cm and are designed not to exceed the elastic range when the structure is subjected to design-intensity earthquakes.

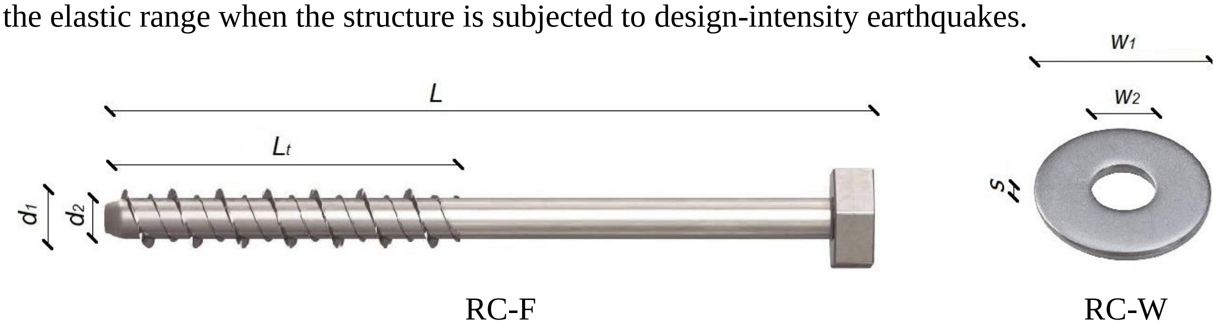


Figure 2: RC frame – timber subframe connection (RC-Conn)

In the last step of the implementation procedure (Figure 1d), a timber panel is inserted inside the RC frame and is connected to the timber subframe by using partially threaded timber screws (CLT-F) and washers (CLT-W) as those represented in Figure 3. This connection is named "T-Conn". In the models described in the present paper, the screws were spaced at 10 cm. The role of the T-Conn is that of transferring the stresses from the timber subframe to the CLT panel and of dissipating seismic energy by engaging the post-elastic behaviour of the fasteners.

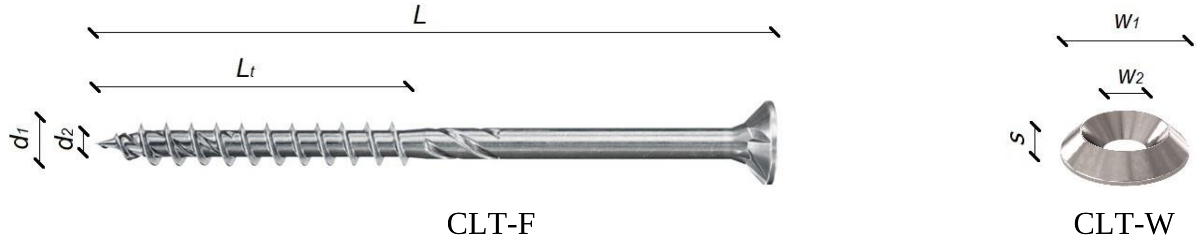


Figure 3: Timber subframe – CLT panel connection (T-Conn)

Table 3 and Table 4 give the geometrical characteristics of screws and washers, respectively.

| | $L$ [mm] | $L_t$ [mm] | $d_1$ [mm] | $d_2$ [mm] |
|---|---|---|---|---|
| RC-F | 200 | 80 | 12,0 | 8,8 |
| CLT-F | 120 | 60 | 10,0 | 6,4 |

Table 3: Geometrical properties for screws

| | $W_1$ [mm] | $W_2$ [mm] | $s$ [mm] |
|---|---|---|---|
| RC-W | 44,0 | 13,5 | 4,0 |
| CLT-W | 30,0 | 10,8 | 6,4 |

Table 4: Geometrical properties for washers

At the perimeter of the CLT panel, between the panel edges and the internal faces of the RC frame there is a gap (visible in Figure 1d). This gap creates the necessary space for the insertion of the panel into the frame and, above all, ensures that the transfer of stress between the frame and the panel is governed by the T-Conn rather than by direct contact. In this way, it is possible to optimize the force-transfer mechanism so as to favour the development of ductile mechanisms (bending) instead of brittle failures (shear).

In the present study, the timber subframe is made of Glued Laminated Timber (grade class GL24h according to [19]) with $b \times h$ dimensions equal to 100 × 120 mm (Figure 1c), while the CLT panel (grade class C24 according to [20]) is 3-layered and 60 mm thick. The mechanical properties and the density of the timber elements are reported in Table 5 and were defined considering the relative Standard Codes [19], [20], and the studies of Bogensperger et al. (2011) [21], Harris et al. (2013) [22] and Gečys at al. (2015) [23].

| | Bending | Tension | | Compression | | Shear | Density |
|---|---|---|---|---|---|---|---|
| | $f_m$ [MPa] | $f_{t,0}$ [MPa] | $f_{t,90}$ [MPa] | $f_{c,0}$ [MPa] | $f_{c,90}$ [MPa] | $f_v$ [MPa] | $\rho$ [kg/m$^3$] |
| GL24h | 24,0 | 19,2 | 0,5 | 24,0 | 2,5 | 3,5 | 420 |
| C24 | 24,0 | 14,5 | 0,4 | 21,0 | 2,5 | 4,0 | 420 |

| | Elastic modulus | | | Shear modulus | | | Poisson ratio | | |
|---|---|---|---|---|---|---|---|---|---|
| | $E_L$ [MPa] | $E_R$ [MPa] | $E_T$ [MPa] | $G_{RL}$ [MPa] | $G_{TL}$ [MPa] | $G_{TR}$ [MPa] | $\nu_{RL}$ | $\nu_{TL}$ | $\nu_{RT}$ |
| GL24h | 11500 | 300 | 300 | 650 | 650 | 65 | 0,00894 | 0,00894 | 0,538 |
| C24 | 11000 | 370 | 370 | 690 | 690 | 69 | 0,0420 | 0,0270 | 0,602 |

Table 5: Mechanical properties and density for the timber elements

Additionally, in case of damage or collapse of the RC frame the use of structural CLT panel leads to a “bearing capacity reserve” for vertical actions. For this reason, the external layers of the CLT panel are oriented along the vertical axis.

## 4 NUMERICAL MODELS

In the present work, two different modelling approaches were used to investigate the RC-TP intervention system. The software Abaqus was used to develop 3-dimensional (3D) refined models (Figure 4a), while the software SAP2000 was used to develop 2-dimensional (2D) simplified models (Figure 4b). Specifically, the refined approach was calibrated based on experimental evidence available from the literature. Subsequently, it was used to investigate the connections implemented in the RC-TP intervention by reproducing them singularly. Furthermore, by using the 3D refined model it was possible to study possible secondary out-of-plane effects that could not have been directly observed with 2D models. The results obtained permitted to calibrate the simpler 2D models to account for the secondary effects with smaller computational effort than that required by the refined models.

Both the refined and the simpler models were used to analyse the above-mentioned RC frame under monotonic in-plane loading considering the bare, the masonry infilled and the retrofitted configurations.

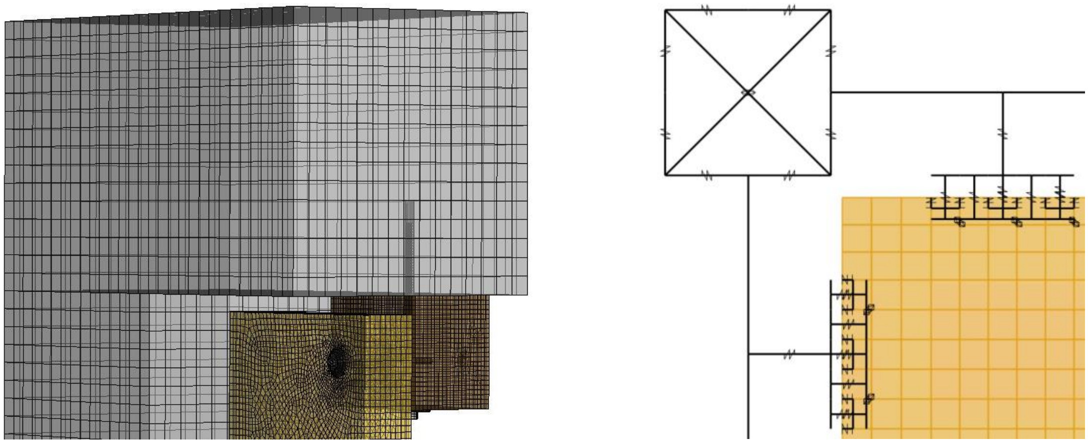

(a) (b)

Figure 4: Alternative numerical approaches: a) Refined 3D Abaqus model; b) Simplified 2D SAP2000 model

### 4.1 3D modelling

The present chapter focuses on the refined 3D modelling strategy used to reproduce the RC-TP intervention system previously described. This strategy was developed using the software Abaqus/Explicit and adopted to perform nonlinear dynamic quasi-static analyses under displacement-control.

In the definition of the analysis steps, the “target time increment” coefficient was calibrated through a sensitivity analysis so as to reduce the processing time to the minimum without affecting the quality of the numerical results.

With the purpose of verifying the absence of dynamic effects, and hence confirm the acceptability of the results, the ratio between internal and kinematics energy was checked a posteriori. As suggested by [24] and [25], this ratio should not exceed 10%. Thanks to the selection of an adequate “time step” and the application of a “smooth” displacement with a sufficiently small initial slope, it was possible to limit the dynamic effects within the predetermined range.

The refined 3D model is represented in Figure 5a. It was obtained by assembling the individual elements that compose the system (a few of these elements are visible in Figure 5b). The geometry of each element was carefully designed and then imported from a 3D CAD [26] environment.

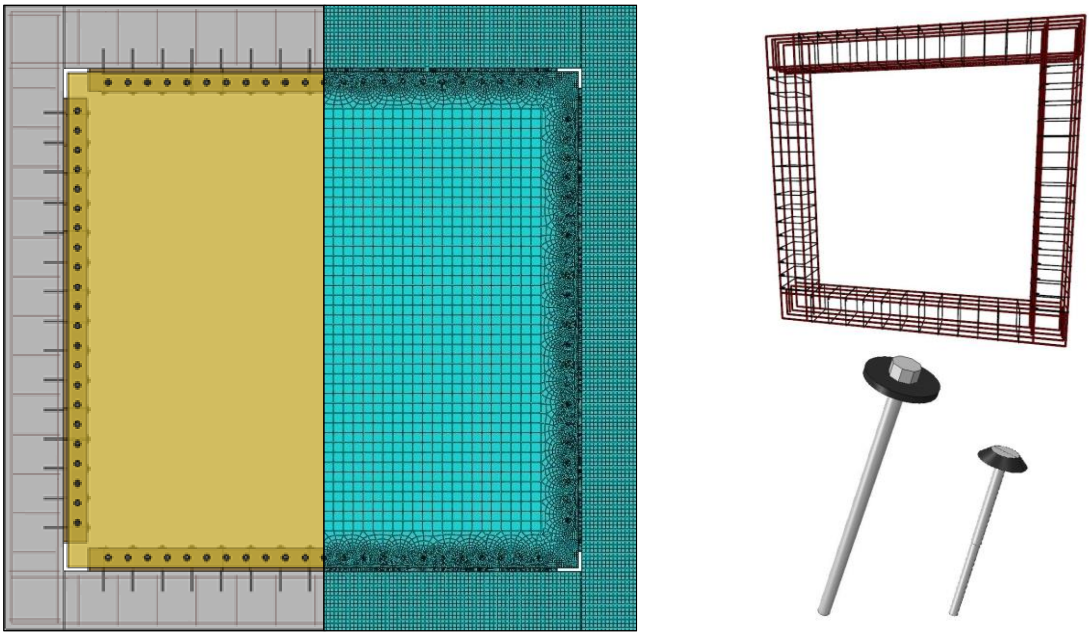

(a) (b)

Figure 5: Intervention system – refined 3D finite element model

Concrete frame, CLT panel, timber subframe, fasteners and washers were all modelled as three-dimensional solid elements (*3D solid part*) with a homogeneous solid section. Steel bars and stirrups, instead, were modelled as one-dimensional elements (*3D wire part*).

Regarding the definition of the materials, the steel elements (bars, stirrups, fasteners and washers) were simulated as isotropic elastic-plastic elements. The three layers that compose the CLT panel were obtained from the division of a single homogeneous solid element and are oriented alternately. Each layer was modelled as an elastic orthotropic material with Hill plasticity, as recommended by [27], where the failure surface was defined with reference to the $f_{c,0}$, $fc_{,90}$ and $f_v$ strength values reported in Table 5. Because of the failure surface symmetry, the positive (tension) stress limit for each principal direction was assumed as identical to the related negative (compression) limit. It was therefore decided to refer to the values associated with the compression parallel and perpendicular to the grain. This choice is justified by the fact that the expected collapse mechanism sees the local bearing failure of the wood material in the proximity of the screw fasteners, which depends almost exclusively on the compressive strength parameters.

The timber subframe was modelled similarly to the layers of the CLT panel (i.e. elastic orthotropic material with Hill plasticity).

The concrete elements were simulated as homogeneous and isotropic, with a post-elastic behaviour based on the "Concrete Damage Plasticity" constitutive law available from the software library, which relies on the material fracture energy for governing the post-peak softening (for more details see [11]). The tension and compression curves for uniaxial loading are reported in Figure 6, where: $\sigma_t - \varepsilon_t$ and $\sigma_c - \varepsilon_c$ are the stress – strain values associated to tension and compression; $E_0$ is the initial elastic modulus; $\sigma_{t0} - \sigma_{c0}$ are the elastic stresses for tension – compression; $\sigma_{cu}$ is the maximum compression stress.

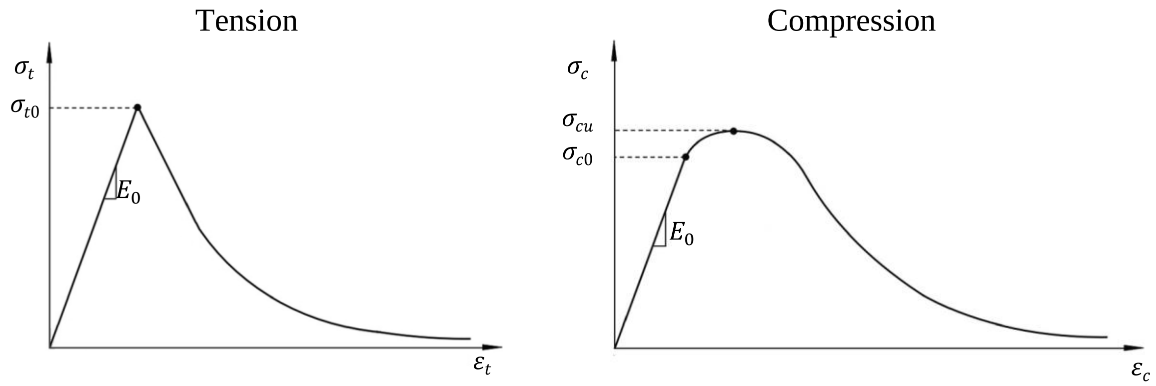


Figure 6: "Concrete Damage Plasticity" behaviour

The interaction between steel reinforcements and frame elements was reproduced with an "Embedded region" constraint (Figure 7). This constraint implies a perfect adherence between the constrained elements.

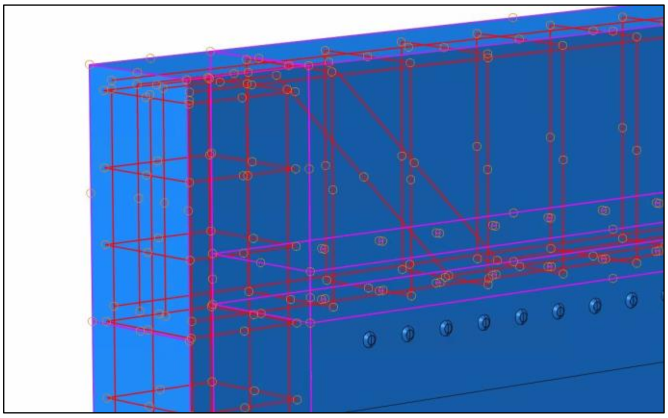

Figure 7: Refined modelling approach – "Embedded region" constraint between concrete and the steel reinforcements

A general "Hard" contact was applied to all the solid elements of the model to avoid unrealistic material penetrations. Additional interaction properties were assigned to the surfaces between the elements ("Individual property assignments") to reproduce the overall behaviour of the system. In particular, a "tangential behaviour" with penalty friction formulation was assigned to the contact surfaces (fasteners-washer, CLT panel-timber subframe, CLT panel-washer, timber subframe-washer, timber subframe-RC frame) using diversified frictional coefficients for the various surface types (e.g., Figure 8 shows the in-contact surfaces between metal fasteners and connected elements).

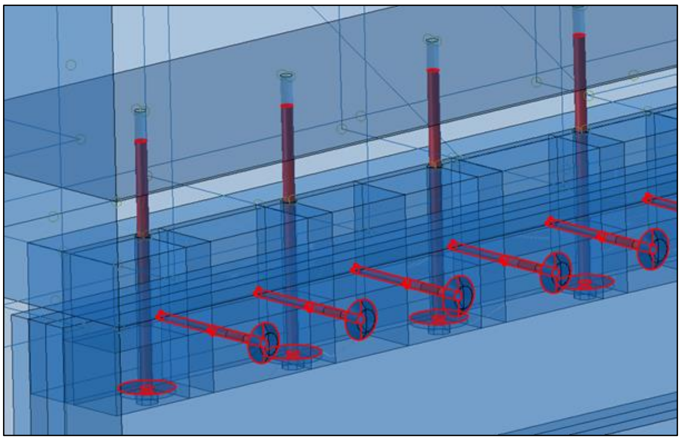

Figure 8: Refined modelling approach – Individual property assignments: fastener cylindrical contact-surfaces

The pull-out mechanisms associated with the threaded portion of the screw fasteners were modelled through a cohesive contact with an elastic uncoupled behaviour depending on $K_n$, $K_s$, $K_t$ (stiffness associated respectively to the normal and the two shear-directions) for which, once the design strength is reached, a damage function reduces the tangential resistance (Figure 9).

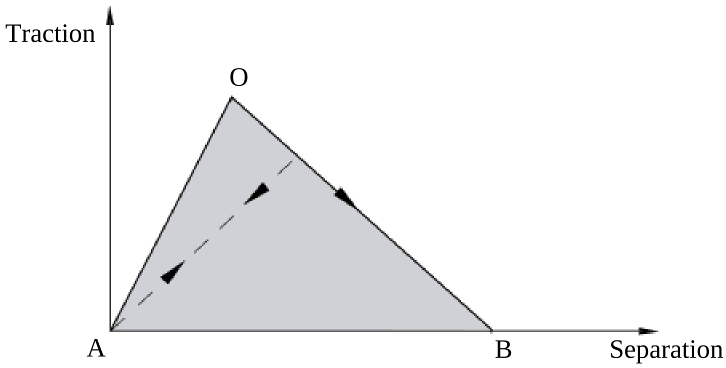


Figure 9: Cohesive fracture energy – damage evolution

To obtained the above mentioned behaviour the "maximum nominal stress" (MAXS) option was selected [27]. As a consequence, the pull-out mechanism activates when Equation 1, which depends on the parameters $t_n$, $t_s$, $t_t$ (normal and shear stresses) and $t_n^0$, $t_s^0$, $t_t^0$ (corresponding reference strength values), is satisfied.

$$max\left\{\frac{t_n}{t_n^0};\frac{t_s}{t_s^0};\frac{t_t}{t_t^0}\right\} = 1 \tag{1}$$

For the modelling of the contacts, the interacting surfaces were categorized into “master” and “slave” surfaces. The mesh characteristics played a fundamental role in the process of attributing the master/slave categories. For all solid components, prismatic “C3D8” elements were preferred to linear tetrahedral elements “C3D4” (which might lead to less reliable results) or quadratic tetrahedral elements “C3D10” (which imply longer analysis durations).

Because the solid models of the RC frame, CLT panel and timber subframe present numerous holes due to presence of the fasteners, it was necessary to partition the geometry to facilitate meshing. Sensitivity analyses were performed and meshes with diverse levels of refinement were adopted for different elements and for different areas in the same element. For example, in the CLT panel, the areas around the fastener holes required a more refined mesh with respect to the rest of the element (Figure 10).

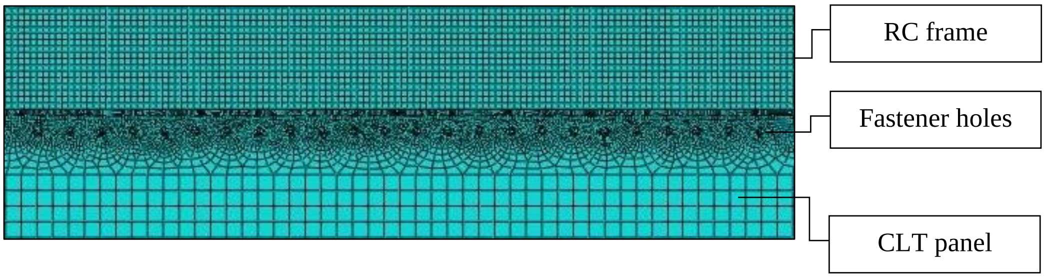


Figure 10: RC-TP refined model – mesh

Once the main aspects of the model were defined, preliminary small-scale analyses were conducted with the aim of calibrating and validating the modelling parameters. The shear and pull-out behaviours of the fasteners were studied separately, considering both the connection with concrete and timber. The numerical results obtained were compared with experimental evidence available from the literature. As an example, Figure 11a and Figure 11b give the comparison between numerical results (red curves) and experimental results taken from [13] (for concrete pull-out) and from [15] (for timber shear) respectively.

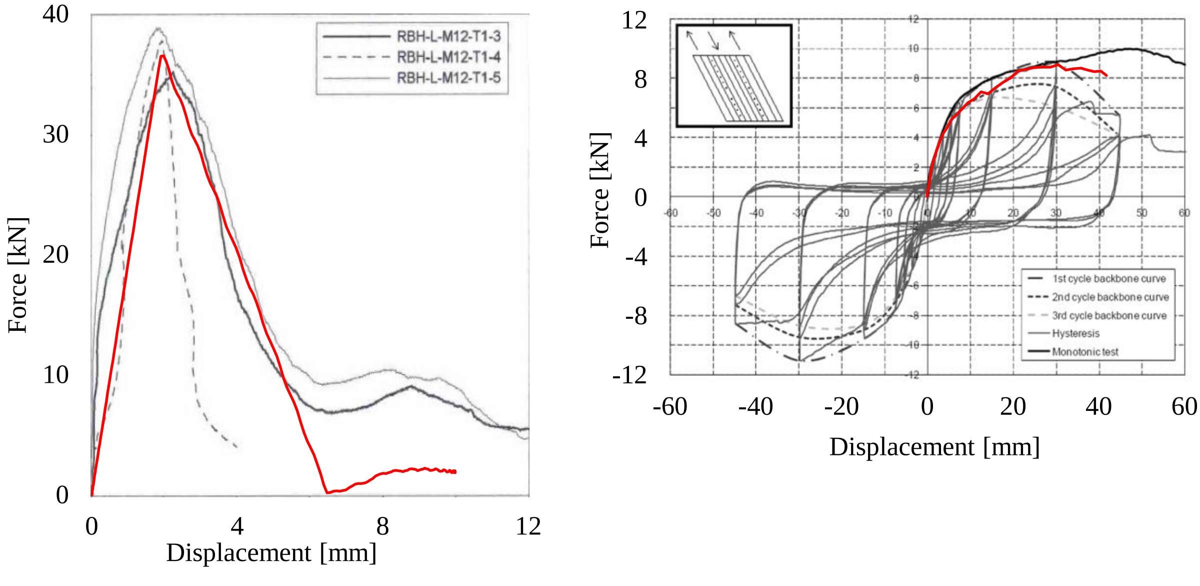


Figure 11: Numerical calibration and validation of the connection behaviour in the refined model (red curves) – comparison with experimental evidence: a) concrete pull-out, b) timber shear

For the original pre-intervention frame configuration, the masonry infill was treated similarly to the concrete elements. Specifically, the infill was modelled with a macro-modelling approach (Figure 12a) where mortar and bricks were represented by an equivalent homogeneous isotropic material (Figure 12b). The post-elastic behaviour was simulated by adopting the "Concrete Damage Plasticity" constitutive model (Figure 6) as suggested by [16]. With this modelling strategy, it is possible to account for both rocking and diagonal shear failure mechanisms. The contact interaction between masonry and concrete is reproduced by a general "Hard" contact and a frictional "tangential behaviour".

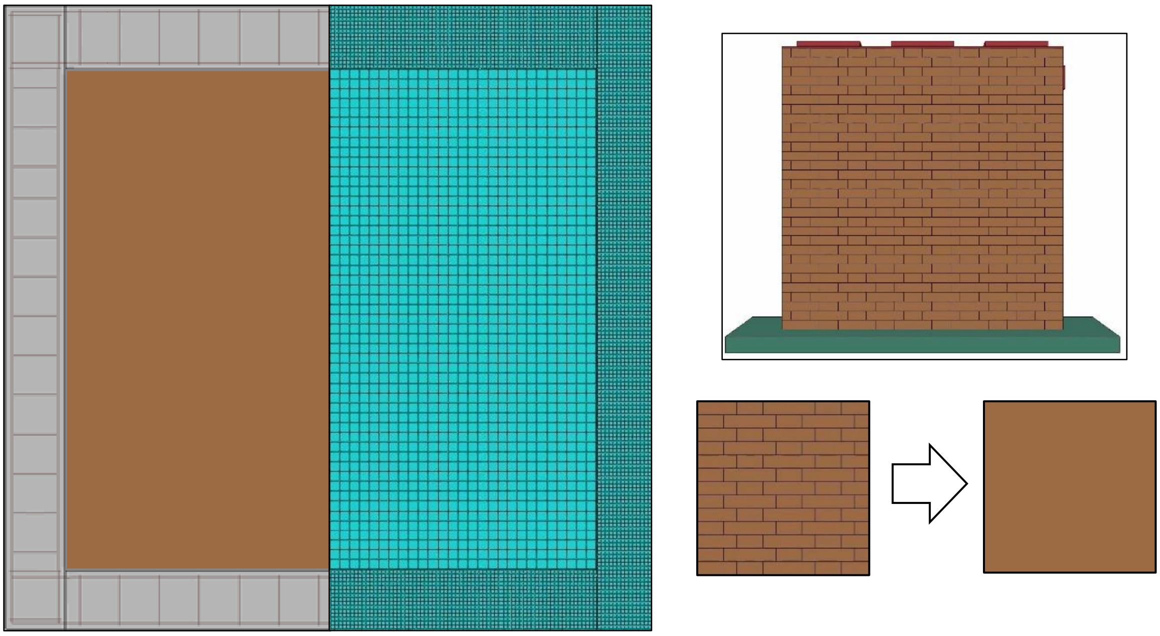

(a) (b)

Figure 12: Refined modelling approach: a) masonry infilled frame; b) mortar and bricks represented as an equivalent homogeneous material

### 4.2 2D modelling

The present chapter focuses on the 2D modelling approaches adopted to simulate the bare frame, the original masonry-infilled frame and the retrofitted frame.

Regarding the retrofitted frame, the modelling strategy presented in this section Figure 13a) is an updated version of that exposed in detail in [9] and [10]. The main upgrades consist in an improved characterization of the non-linear properties of the elements and in an improved definition of the behaviour of the connections. By relying on the findings of the 3D refined models, the 2D approach was calibrated to account for possible out-of-plane secondary effects. The main characteristics of the 2D models are summarized in the following paragraphs.

The concrete frame was modelled by using *frame elements* capable of accounting for the nonlinear behaviour of concrete and steel. Deformation-controlled and force-controlled *hinge elements* were assigned at the extremities of columns and beams to consider respectively bending and shear collapse.

The nonlinear response of the beam-column joint was simulated by using two cross *nonlinear links* connected to the extremities of columns and beams. The joint model adopted herein has been proposed by Sung et al. (2013) [28] and it permits to account for the failure of the joints with small computational effort.

The CLT panel was modelled via *layered orthotropic nonlinear shell elements* where each of the three layers was assumed to be "inactive" along its weak direction.

The timber subframe was an *elastic frame element*. The validity of the elastic-behaviour assumption was confirmed a posteriori by investigating the subframe stress state.

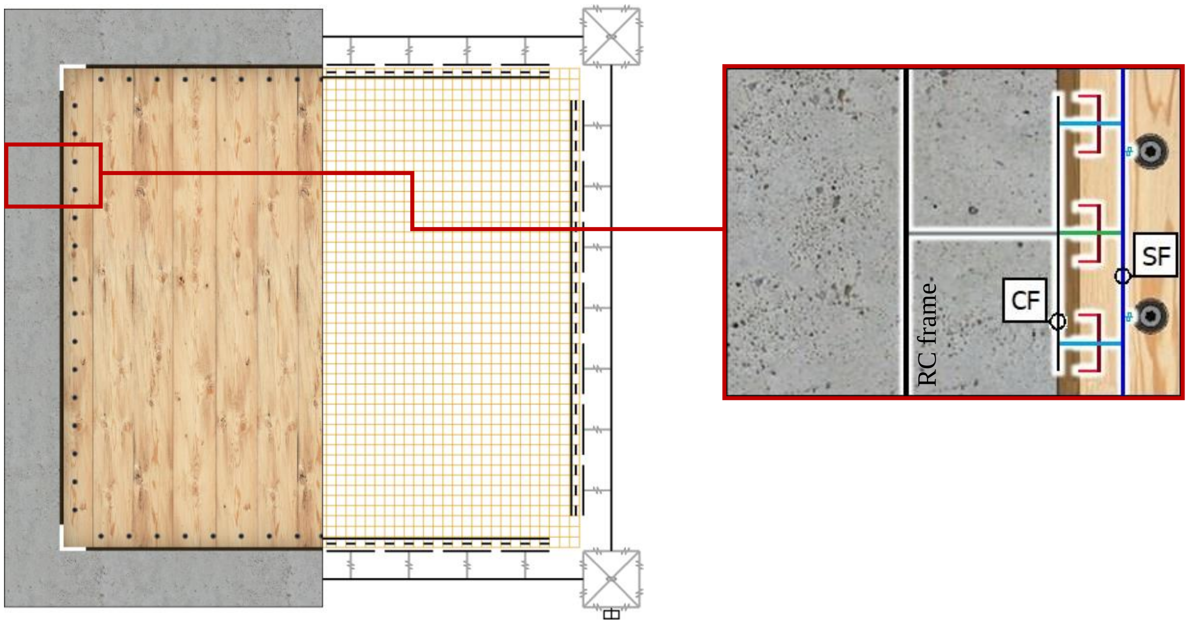


(a) (b)

Figure 13: Simplified finite element model: a) Complete intervention system; b) Interaction system

As extensively described in [10], an “interaction system” reproduces the interaction between RC frame, timber subframe and CLT panel. In Figure 13b, it is possible to observe the frame elements that represent the middle line of the column “RC frame”, the internal face of the column “CF” and the middle line of the timber subframe “SF”.

The interaction system (Figure 13b and Figure 14a) is obtained from the overlap of a “connection system” and a “contact system”.

The connection system (Figure 14b) simulates the RC-Conn (represented by the *link elements* “CL”) and the T-Conn (represented by the *link elements* “TL”). In addition, this system simulates the contact-interaction between the timber subframe “SF” and the internal face of the concrete frame “CF”. This contact is governed by *gap link elements* “GL”.

The contact system (Figure 14c) replicates the direct contact between CLT panel and RC frame. This contact occurs when the gap between the CLT panel and the internal face of the RC frame (CF) goes to zero and it is reproduced by using *hook link elements* “HL”.

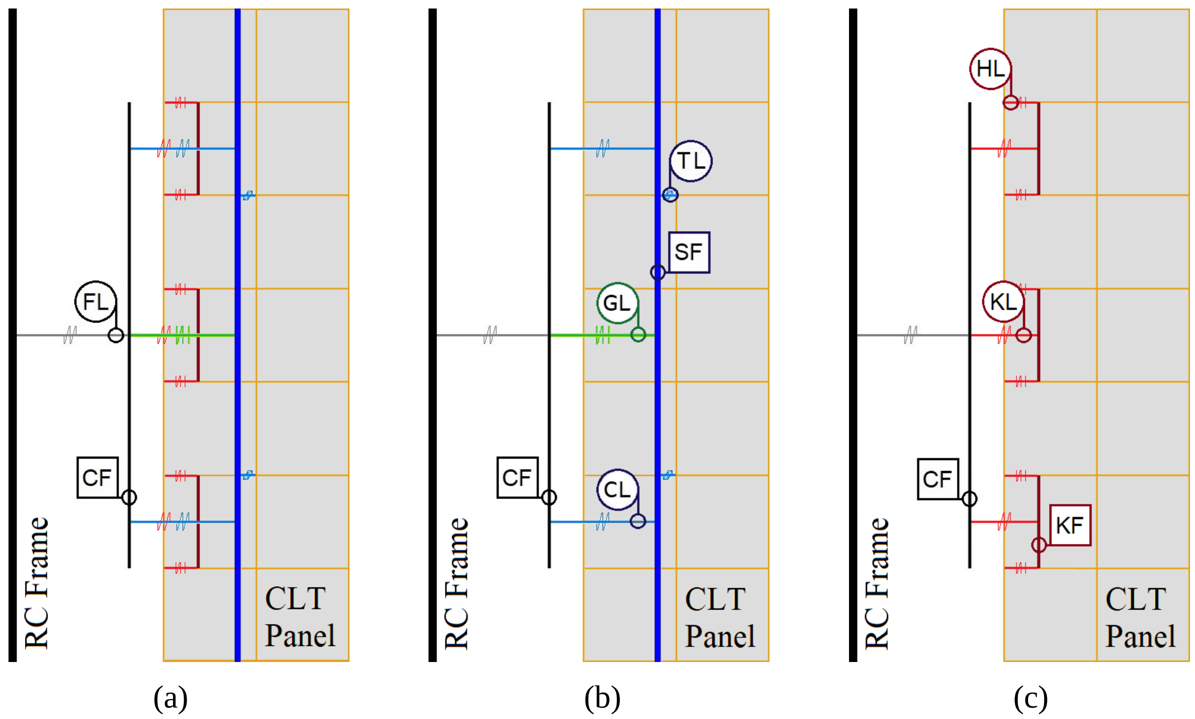


Figure 14: Interaction system between RC frame, timber subframe and CLT panel: (a) Complete interaction system; (b) connection system; (c) contact system

Table 6 reports a summary of the abbreviations used for the main elements and a brief description of the relative functions.

| ID | Name | Functions |
|---|---|---|
| CF | Concrete Frame | - Massless rigid frame.<br>- Represents the internal surface of the RC elements. |
| KF | Fake Frame | - Massless rigid frame.<br>- Used as a support element in the contact system. |
| SF | Subframe Frame | - Elastic frame.<br>- Geometrical characteristics of the timber subframe.<br>- Positioned on the middle line of the timber subframe. |
| CL | Concrete fastener Link | - Nonlinear link.<br>- Represents the RC-Conn. |
| FL | Frame-thickness Link | - Rigid link<br>- Represents the in-plane semi-thickness of column and beams. |
| GL | Gap Link | - Nonlinear gap link.<br>- Reproduces the contact between RC frame and timber subframe. |
| HL | Hook Link | - Nonlinear hook link.<br>- Reproduces the contact between timber subframe and CLT panel. |
| KL | Fake Link | - Rigid link.<br>- Used as a support element in the contact system. |

| | | |
|---|---|---|
| TL | Timber fastener Link | - Nonlinear link.<br>- Represents the T-Conn.. |

Table 6: Interaction system – Abbreviations used and main functions

The nonlinear behaviour of CLs and TLs was defined based on the results obtained from the refined Abaqus 3D models because such models account for possible effects due to the out-of-plane eccentricity associated with the physical thickness of the various components. The details of the curves assigned to the CLs and TLs are given in the next section.

The response of the original masonry infilled system was simulated by using an equivalent diagonal struts model (Figure 15). This model was defined starting from the approaches proposed by Al-Chaar (2002) [17] and Liberatore et al. (2018) [18]. Specifically, the proposed masonry model consists of two eccentric diagonal rods, whose location in the RC frame is given by the provisions of [17], while the compression behaviour of the rods is defined according to [18]. The tensile strength of the diagonal elements reproduces the tensile strength of the masonry. Consequently, if a lateral force is applied as shown in Figure 15a, the two links work as strut and tie. The behaviour of each diagonal link is reported in Figure 15b, where the blue branch and the red branch represent the compression and the tension response respectively.

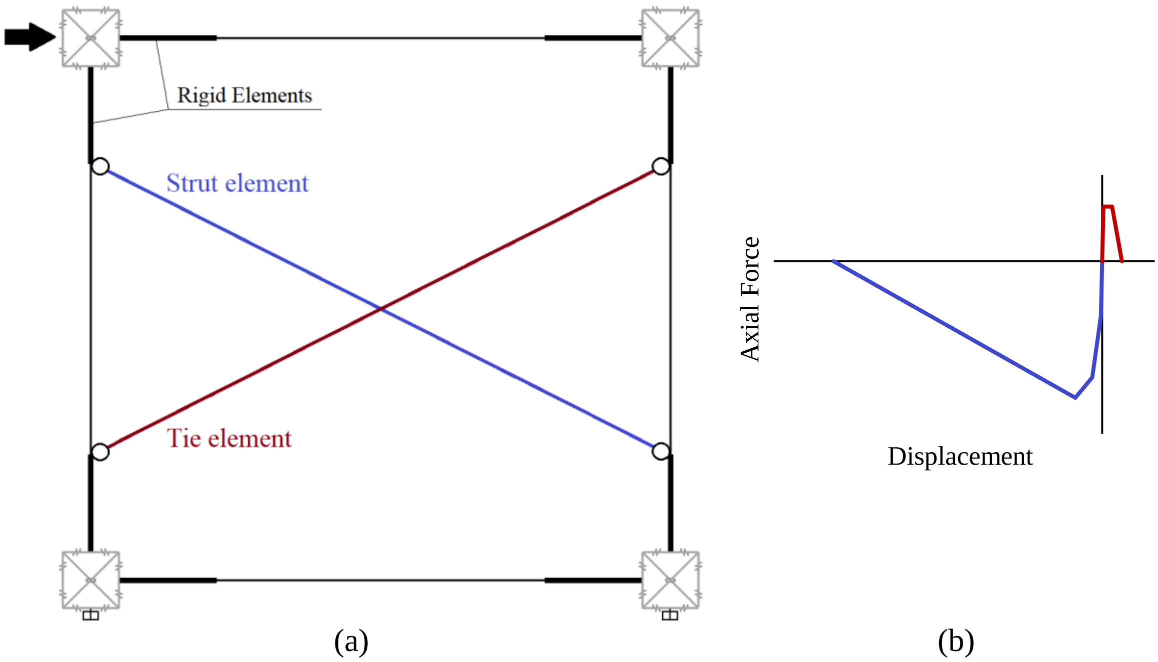


Figure 15: Original masonry-infilled system: a) Equivalent diagonal "strut and tie" model; b) Force-displacement response

According to [17], in order to consider the confinement produced by the masonry infill, the portions of beams and columns between the joints and the diagonal links are modelled as *rigid elements* (Figure 15a). Only the intermediate sections of columns and beams can therefore develop nonlinear responses.

## 5 NUMERICAL ANALYSES AND RESULTS

### 5.1 Preliminary analyses

The first step of the numerical study presented herein saw the simulation of isolated RC-Conn and T-Conn connections under pull-out and shear loading conditions. Several configurations were considered (e.g., pull-out tests carried out by pulling the screw directly or by pulling the subframe, or shear and pull-out tests performed “with and without” washers). Figure 16 shows the most relevant results: a) RC-Conn - push-out; b) RC-Conn - shear parallel to the subframe; c) T-Conn - shear perpendicular to the subframe; d) T-Conn - shear parallel to the subframe.

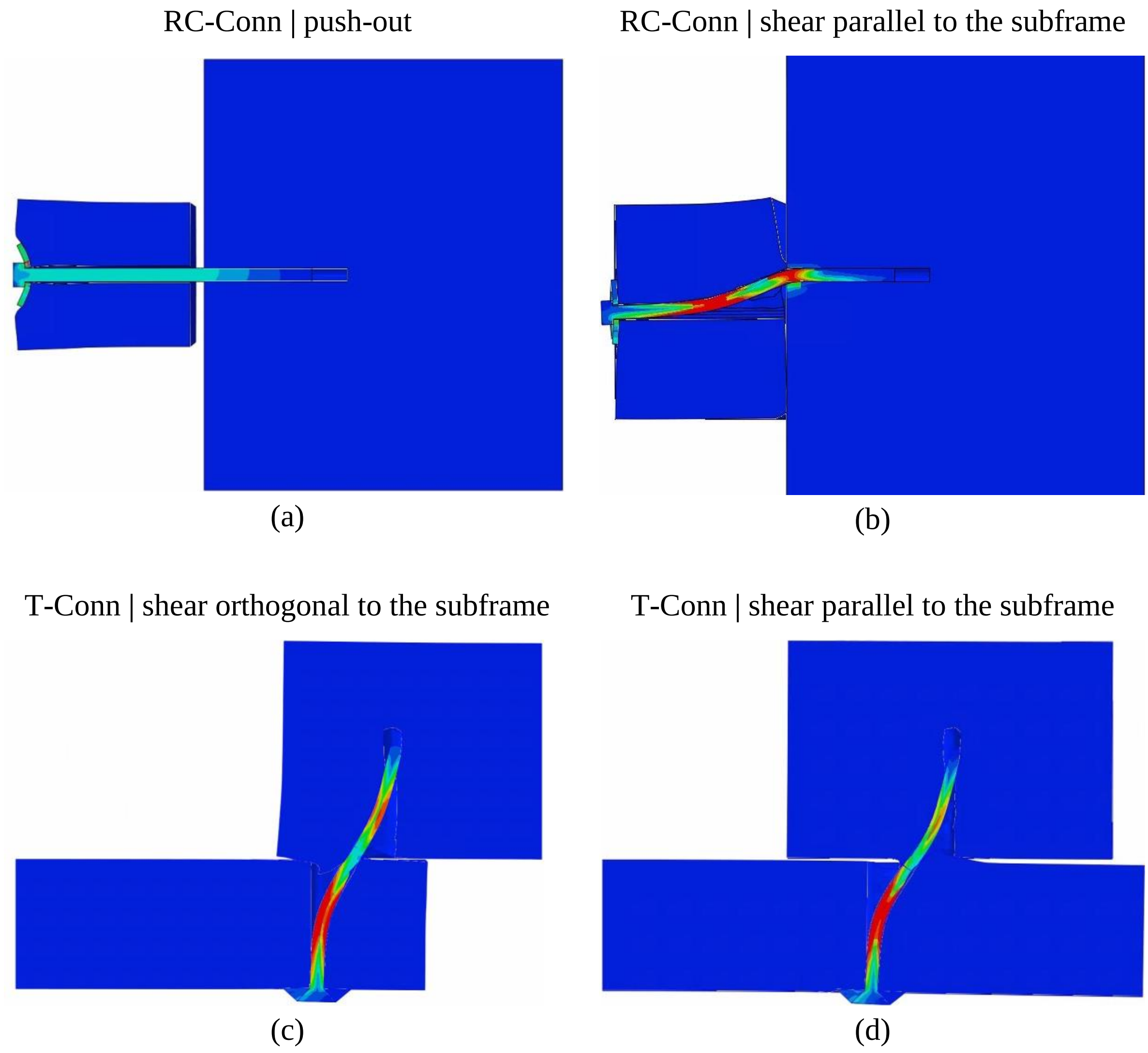


Figure 16: Tests on RC-Conn and T-Conn – stress contour

Subsequently, in order to account for possible out-of-plane displacements due to the eccentrical interaction between RC frame – timber subframe – CLT panel, a test structure (referred to as "Test-Module") was defined (Figure 17). The size of the Test-Module was selected so as to replicate the “base-unit” of the retrofit system. Because the RC-Conns have a 15 cm spacing and the T-Conns have a 10 cm spacing, the Test-Module comprise two RC-Conn and three T-Conn fasteners.

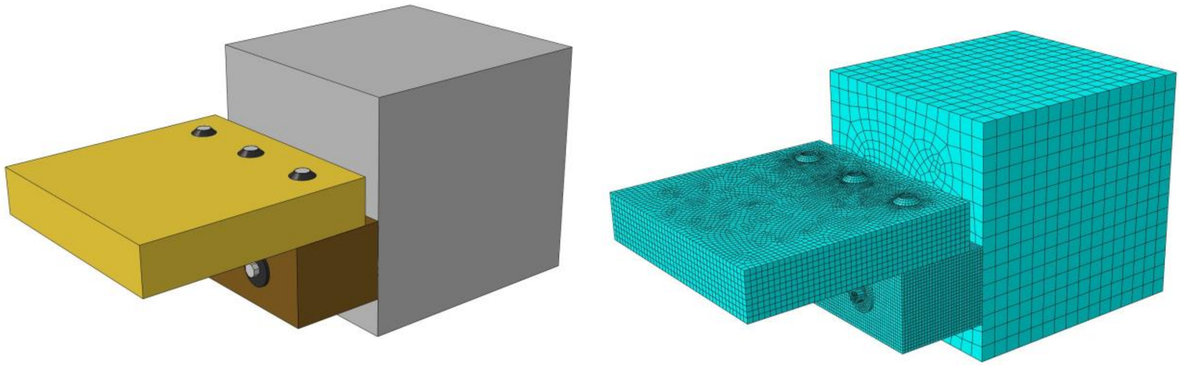

Figure 17: “Test-Module”

The out-of-plane effects observed from the analysis of the Test-Module were included in the simplified 2D models through the response-curve attributed to the TL and the CL elements (for labelling details please see Table 6). In particular, such secondary effects were found to be non-negligible when the force was applied in the Z-direction (Figure 18a).

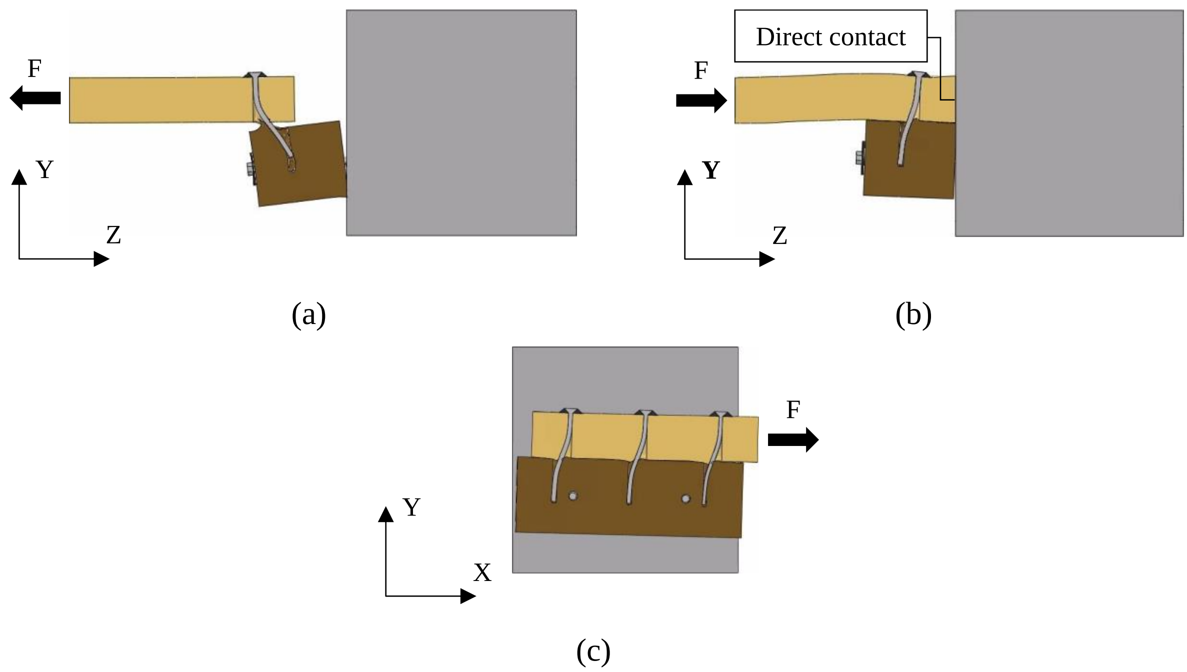


Figure 18: “Test-Module” – out-of-plane secondary effects

Figure 19 shows the backbone curves of the T-Conn shear tests (Figure 19a) and RC-Conn pull-out tests (Figure 19b). The green curves were obtained from the 3D model neglecting the secondary effects by restraining the out-of-plane movements. The blue curve obtained with the refined model considering the secondary effects. The red curves, which are the idealized versions of the blue curves, were subsequently implemented in the 2D model to account for the secondary effects.

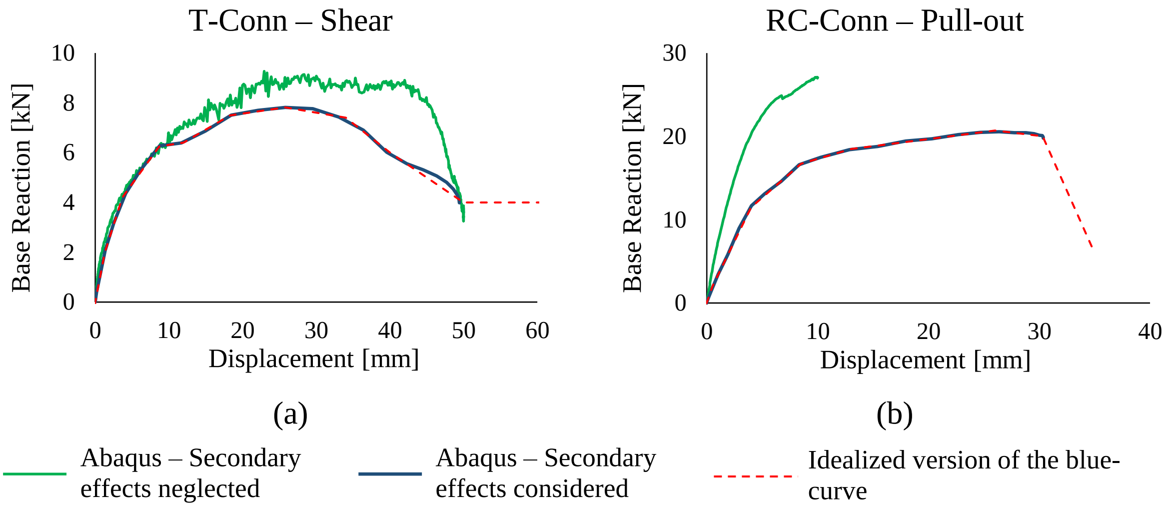


Figure 19: Backbone curves from single-connection tests: a) T-Conn shear; b) RC-Conn pull-out

Figure 20 shows the response of the Test-Module obtained by using the 3D refined modelling approach and the 2D modelling approach (with secondary effect accounted for). In particular, in Figure 20a, the force applied to the panel was parallel to the X-direction (Figure 18c), while in Figure 20b the panel was pulled and pushed in the Z-direction (see Figure 18a and Figure 18b).

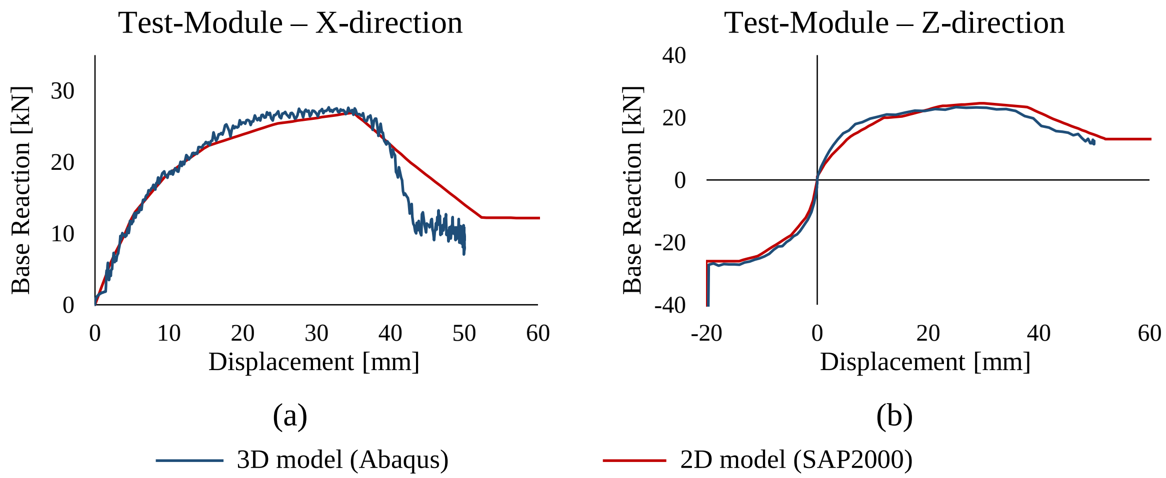


Figure 20: Behaviour of the Test-Module obtained with the 3D (blue) and the 2D (red) approach: a) X direction; b) Y direction

As it is possible to observe from the graphs, the outcomes of the two modelling approaches are consistent for both test configurations. When including the out-of-plane secondary effects in the 2D model, it was possible to match closely the curves from the 3D model at a much smaller computational effort. As visible from Figure 20b, it is interesting to notice that both the 3D and the 2D models experienced a sudden stiffness increase at a negative displacement close to –20 mm. This increase is due to the gap between the CLT panel and the RC frame (represented by the HL elements in the 2D model) that goes to zero involving a direct contact (observable from Figure 18b).

### 5.2 Full-scale one-storey one-bay frame

After having calibrated the 2D modelling approach on the results from the connection tests studied with the 3D approach, and having proof-checked the correspondence between the approaches through the analysis of the Test-Module, the case-study frame described in section 2 was modelled.

The one-storey, one-bay frame was analysed considering three alternative configurations: Bare frame (Figure 21a), Masonry infilled frame (Figure 21b) and RC-TP retrofitted frame (Figure 21c). Based on the findings reported in [9] and [10], the optimal RC-TP configuration for the case-study frame was assumed to be that having a GAP of 20 mm and T-Conns arranged only along the beams.

The three frame configurations were analysed with both modelling approaches via nonlinear static analysis. In the first step, the vertical loads (values reported in Table 2) were applied to the columns and the upper beam. Then, the in-plane horizontal force was introduced at the top joint level and was incremented until the collapse of any of the structural elements was reached.

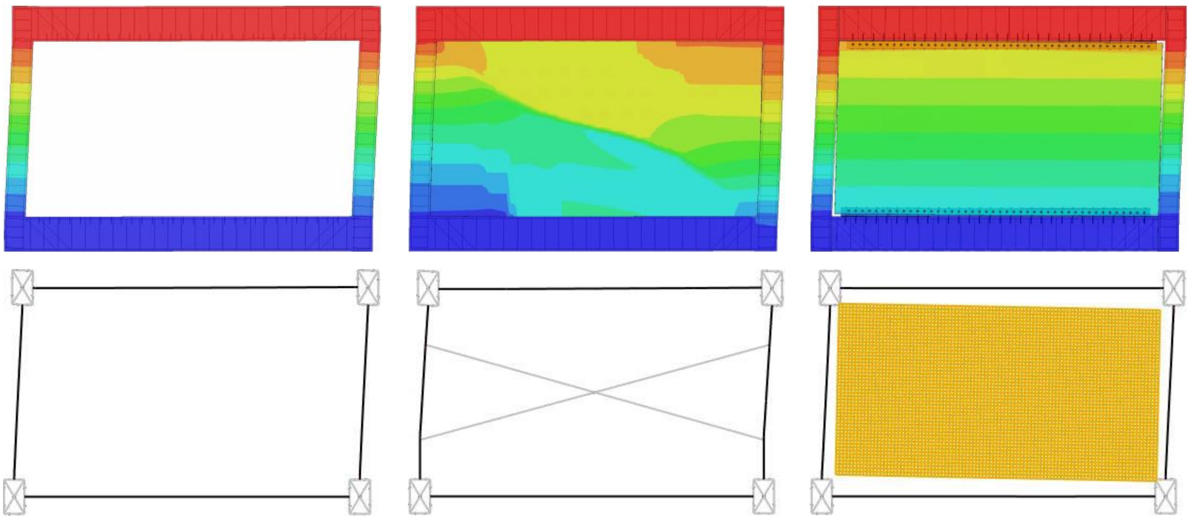

(a) (b) (c)

Figure 21: 3D and 2D models of the case-study frame configurations: a) Bare frame; b) Masonry infilled frame; RC-TP retrofitted frame

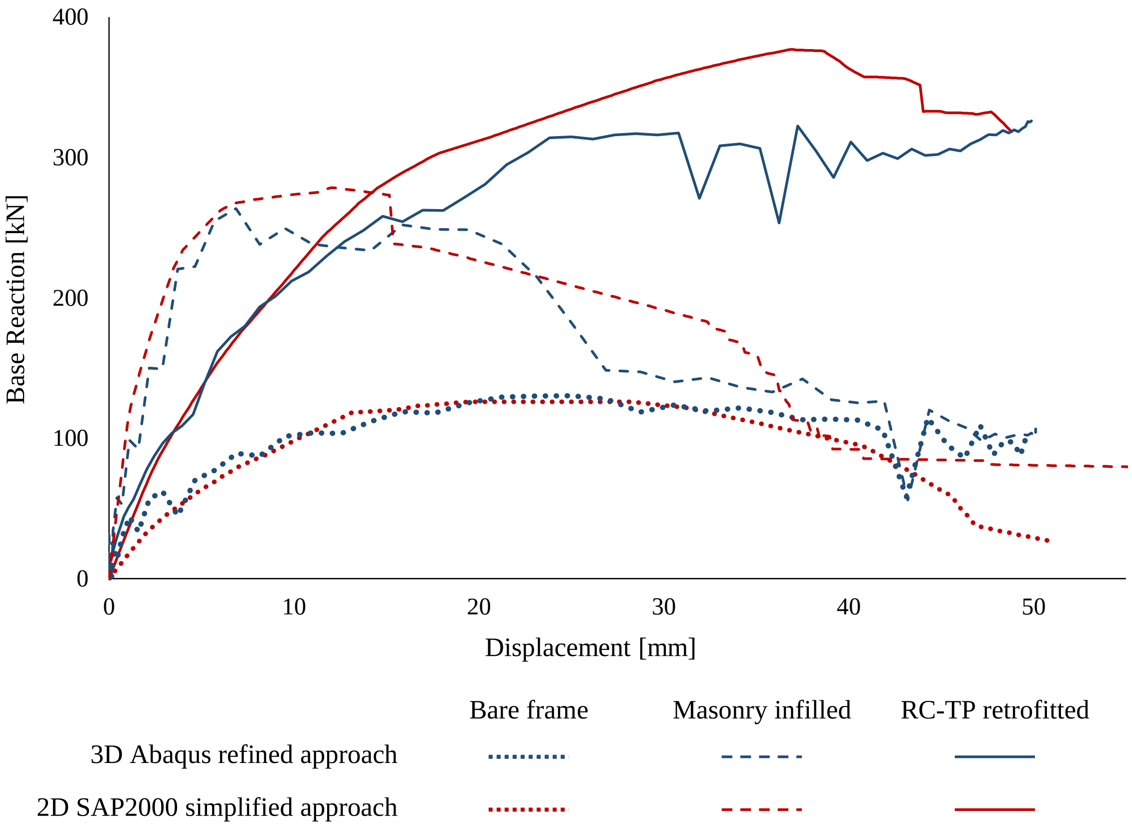


Figure 22: Isolated frame backbone curves – comparison between the 3D and the 2D modelling approach

Figure 22 reports the results obtained by performing the nonlinear static analyses of the isolated frame in the three configurations and using both modelling approaches. Both numerical strategies produced consistent results, showing similar behaviours for all the analysed configurations in terms of stiffness, strength and failure mechanism.

For all three configurations the frame collapsed due to the bending failure of the concrete column. However, for the masonry infilled frame, the column failure was preceded by the collapse of the infill which caused an evident reduction in the load bearing capacity at a displacement level close to 20 mm. The retrofitted frame, instead, showed a remarkable increase in the bearing capacity, with the peak capacity at a displacement of approximately 40 mm. The bending failure of the concrete columns in the retrofitted frame occurred at displacement values similar to those observed in the bare frame, attesting that the proposed intervention does not impede the full development of the column flexural ductility.

## 6 CONCLUSIONS

The present paper reports the results of a numerical study on a retrofit intervention for existing RC masonry infilled structures. The intervention, named RC-TP, is aimed at reducing the seismic vulnerability of this kind of structure by replacing the masonry infills with timber panels connected to the RC-frame with screw-fasteners. The present research focused on the modelling of the pre- and post- intervention system via two alternative numerical strategies with different levels of refinement. In particular, a 3D refined modelling approach and a 2D simpler modelling approach were investigated. Preliminary analyses on isolated connections permitted both to validate the 3D modelling approach on experimental evidence available from the literature, and to calibrate the 2D models to account for secondary effects that cannot be directly observed by two-dimensional models. Consequently, an isolated one-storey one-bay concrete frame representative of the built stock of many Countries was modelled using both strategies and considering the “bare”, the “masonry infilled” and the “retrofitted” configurations. The RC frame was subjected to nonlinear static analyses until the collapse of any of the structural elements was reached. The analysis outcomes showed that the proposed retrofit system can effectively reduce the seismic vulnerability of existing masonry infilled RC frames, consistently with the findings of preliminary studies previously published. By virtue of the good correspondence between the refined 3D approach and the less refined but computationally far more efficient 2D approach, future steps of the research will be devoted to using the 2D models for extensive parametric studies on all the details affecting the performance of the timber-panel strengthening technique discussed herein.

## 7 ACKNOWLEDGEMENTS

The research work was carried out within the framework of the 2019-2021 ReLUIS-DPC network (Italian University Network of Seismic Engineering Laboratories and Italian Civil Protection Agency).

**REFERENCES**


[1] S. Kadysiewski and K.M. Mosalam KM. Modeling of Unreinforced Masonry Infill Walls Considering In-Plane and Out-of-Plane Interaction. Pacific Earthquake Engineering Research Center, University of California, Berkeley, California, 2009

[2] M. Gaetani d'Aragona, M. Polese,M. Di Ludovico,A. Prota. Seismic vulnerability for RC infilled frames: simplified evaluation for as-built and retrofitted building typologies. *Buildings*, 8(10):137, 2018

[3] D. Perrone, M. Leone, M.A. Aiello. Non-linear behaviour of masonry infilled RC frames: influence of masonry mechanical properties. *Eng Struct*, 150 (2017), pp. 875-891, 2017

[4] N. Ning, Z. John Ma, P. Zhang, D. Yu, and J. Wang. Influence of masonry infills on seismic response of RC frames under low frequency cyclic load. *Engineering Structures*, vol. 183, pp. 70–82, 2019

[5] I. Sustersic and B. Dujic. Seismic strengthening of existing buildings with cross laminated timber panels. *World Conference on Timber Engineering*. Auckland, New Zeland, 16-19 July, 2012.

[6] J. Suga, M. Ono, K. Aoki, T. Fukuhara, T. Kurihara, T. Maeda. Timber Shear Walls for Seismic Retrofit of Reinforced Concrete Buildings. *World Conference on Timber Engineering*. Seoul, Republic of Korea, 20-23 August; 2018

[7] F. Staz, M. Serpilli, G. Maracchini, A. Pavone. An experimental and numerical study on CLT panels used as infill shear walls for RC buildings retrofit. *Construction and Building Materials*, 211: 605-616. https://doi.org/10.1016/j.conbuildmat.2019.03.196, 2019

[8] G. Margani, G. Evola, C. Tardo, and E.M. Marino. Energy, Seismic, and Architectural Renovation of RC Framed Buildings with Prefabricated Timber Panels. *Sustainability*, 12, p. 4845, 2020

[9] F. Smiroldo, I. Giongo, M. Piazza. Seismic retrofit of masonry infilled frames by using timber panels. *17th World Conference on Earthquake Engineering, 17WCEE*, Sendai, Japan, 2020.

[10] F. Smiroldo, I. Giongo, M. Piazza. Use of timber panels to reduce the seismic vulnerability of concrete frame structures. *Engineering Structures*, 2021.

[11] Dassault Systèmes: Abaqus analysis users' manual, Simulia Corp., Providence, RI, USA, 2011

[12] SAP 2000 Integrated Software for Structural Analysis and Design, Computers and Structures Inc., Walnut Creek,California, USA.

[13] M. Madeddu. Preliminary tests on Screw Anchor. *Polytechnic University of Milan – Department of Structural Engineering - Testing Material Laboratory – CE Marking Section*, 2006.

[14] R. Tomasi, A. Crosatti, M. Piazza M. Theoretical and experimental analysis of timbertotimber joints connected with inclined screws, *Constr Build Mater*, 24:1560–71, 2010

[15] I. Gavric, M. Fragiacomo, A. Ceccotti. Strength and deformation characteristics of typical CLT connections. *Proceeding of the 12th World Conference on Timber Engineering*, Auckland, New Zealand, 2012

[16] P. Lourenco, Structural masonry analysis: recent developments and prospects. *Proceedings of the 15th International brick & brick masonry conference*, Sydney, Australia, 1341-1356, 17-20 February 2008.

[17] G. Al-Chaar, Evaluating Strength and Stiffness of Unreinforced Masonry Infill Structures, *407 US Army Corps of Engineers*, *Engineer Research and Development Center*, ERDC/CERL TR-408 02-1, Illinois, 2002

[18] L. Liberatore, F. Noto, F. Mollaioli and P. Franchin. In-plane response of masonry infill walls: Comprehensive experimentally-based equivalent strut model for deterministic and probabilistic analysis. *Engineering Structures*, 167: 533-548. https://doi.org/10.1016/j.engstruct.2018.04.057, 2018

[19] EN 14080:2013. Timber Structures – Glued laminated timber and glued solid timber – Requirements, *European Committee for Standardization*, Brussels.

[20] EN 338:2016. Structural timber – Strength classes, *BSI Standards Publication*, London, UK.

[21] T. Bogensperger, M. Augustin, G. Schickhofer, *Properties of CLT-panels exposed to compression perpendicular to their plane*. 44th CIB-W18 Meeting, Alghero, 2011

[22] R. Harris, A. Ringhofer and G. Schickhofer. Focus Solid Timber Solutions – European Conference on Cross Laminated Timber (CLT). *Institute of Timber Engineering and Wood Technology (2 676 080)*, University of Bath, UK, 2013.

[23] T. Gečys, A. Daniūnas, T.K. Bader, L. Wagner, J. Eberhardsteiner, 3D finite element analysis and experimental investigations of a new type of timber beam-to-beam connection. *Engineering Structures*, 86, 134–145, 2015

[24] Y. Hu, L. Shen, S. Nie, B. Yang, W. Sha. FE simulation and experimental tests of high-strength structural bolts under tension. *Journal of Constructional Steel Research*, 2016

[25] A. Al-Rifaie, Z.W. Guan, S.W. Zones. Quasi-Static Analysis of End Plate Beam-to-Column Connections. *Engineering and Technology*, *International Journal of Civil and Environmental Engineering*, Vol:11, No:7, 2017

[26] AutoCAD, Autodesk, Inc., California, USA.

[27] C. Bedon, M. Fragiacomo, Numerical analysis of timber-to-timber joints and composite beams with inclined self-tapping screws. *Composite Structures* 207, 13–28, 2019

[28] Y.C. Sung YC, T.K. Lin, C.C. Hsiao and M.C. Lai, Pushover analysis of reinforced concrete frames considering shear failure at beam-column joints. *Earthquake Engineering and Engineering Vibration*, 12 (3), 373-383, 2013